Soft Matter

RSC Publishing

PAPER

View Article Online
View Journal | View Issue

Thermo-responsive peptide-based triblock copolymer hydrogels†

Cite this: *Soft Matter*, 2013, **9**, 4304

Antoni Sánchez-Ferrer,‡[a] Venkata Krishna Kotharangannagari,‡[ab] Janne Ruokolainen[c] and Raffaele Mezzenga*[a]

Received 21st November 2012
Accepted 7th February 2013

DOI: 10.1039/c3sm27690b

www.rsc.org/softmatter

A series of novel thermo-responsive peptide-based triblock copolymers, poly(L-glutamic acid)-*b*-poly(*N*-isopropylacrylamide)-*b*-poly(L-glutamic acid) (PLGA-*b*-PNIPAM-*b*-PLGA), were successfully synthesized *via* ring opening polymerization (ROP) of the γ-benzyl L-glutamate derivative (BLG-NCA) using a diamino-terminated PNIPAM as a macroinitiator, followed by de-protection of the benzyl groups. These triblock copolymers form physically crosslinked networks after complexation with a diamino-terminated poly(ethylene oxide) (PEO) in an organic solvent through acid–base proton transfer and successive ionic-bonding confirmed by Fourier transform infrared (FTIR) spectroscopy. The secondary structure of the peptide block, before and after complexation, was confirmed by circular dichroism (CD) experiments, showing an α-helix conformation of the PLGA segments. Swelling experiments on the ionic-bonded networks showed that the water uptake process strongly depends on the temperature and relative humidity conditions. Thus, higher humidity and temperatures below the lower critical solubility temperature (LCST) of the PNIPAM block increase the amount of water absorbed into the network. These swollen ionic complexes contract and reject water when these thermo-responsive peptide-based hydrogels are heated up above their LCST, making them promising for biomedical applications and drug delivery systems.

Introduction

Hydrogels are physically and/or chemically crosslinked three-dimensional polymeric networks that absorb large amounts of water. These kinds of materials have gained great interest during the last few decades due to their excellent biocompatibility and capability to absorb and release molecules during the swelling–deswelling processes, which make them very attractive for biomedical applications such as tissue engineering scaffolds, drug delivery carriers, and biomedical devices.[1–8]

Moreover, stimuli-responsive hydrogels are very appealing systems because of their reversibility when sol–gel transition or volume phase transition occurs in response to external physical or chemical stimuli, such as pH, temperature, ionic strength, a magnetic field, and light.[9–13]

Among the stimuli-responsive hydrogels, thermo-responsive hydrogels are some of the most widely used physical stimuli-responsive hydrogels and are very useful for biomedical application as an injectable hydrogel.[14,15] Poly(*N*-isopropyl acrylamide) (PNIPAM) is one of the most popular thermo-responsive polymers with a lower critical solution temperature (LCST) around 32 °C, which makes PNIPAM-based hydrogels very useful model systems for biomedical applications since its LCST is close to body temperature (37 °C).[5,10,16–18]

Polypeptides are attractive macromolecules in the biomedical field due to their unique protein-mimetic properties,[19–22] and thermo-responsive peptide-based hydrogel systems are capable of undergoing reversible sol–gel processes which could target unchallenged potential applications not only in the biomedical field, but also in the area of drug delivery due to the desirable combined effect of non-invasive stimuli-responsiveness and biocompatibility.[23,24]

However, in the case of peptide-based hydrogel systems, the gel formation is typically through non-covalent interactions such as hydrogen bonding, π–π stacking, van der Waals and solvophobic interactions.[25,26] Small peptide-based gels have been shown to form molecular fibril networks, and have shown thermo-reversibility and pH responsiveness.[27,28] Peptide-based rod-coil diblock copolymers can form hydrogels with potential applications in biotechnology.[29–31] Moreover, in peptide-based block copolymers, gels can be further tuned by ionic interactions, coil–coil interactions or hydrophobic association.[32–34]

[a]*ETH Zurich, Food & Soft Materials Science, Institute of Food, Nutrition & Health, Schmelzbergstrasse 9, LFO, E23-29, CH-8092 Zürich, Switzerland. E-mail: raffaele.mezzenga@hest.ethz.ch*

[b]*Department of Physics, Frimat Center for Nanomaterials, University of Fribourg, Chemin du Museé 3, CH-1700 Fribourg, Switzerland*

[c]*Department of Applied Physics, AALTO University, P. O. Box 15100, FI-00076 Helsinki, Finland*

† Electronic supplementary information (ESI) available: Detailed experimental procedures, sample preparation, FTIR and CD spectra, WAXS experiments, as well as swelling experiments of the ionic complexes IC1 and IC2. See DOI: 10.1039/c3sm27690b

‡ The first two authors contributed equally to this study.

In the past few years, great attention has been paid to the development of peptide-based stimuli-responsive hydrogels because they have excellent biocompatibility and the resulting materials can be used in biomedical applications, such as drug delivery systems.[6] Very recently, a pH and thermo-responsive polypeptide-based hydrogel was described, which was obtained from normal and reverse micelles *via* the cooperation of host-guest chemistry and hydrogen-bonding interactions controlling the drug-release behaviour.[35]

In order to develop new hydrogels, two parameters have been considered, temperature and biocompatibility, which are essential for biomedical applications in which injectable hydrogels are the desired active material. Taking into account and being inspired by the state of the art hydrogels, a combination of a polypeptide with a thermo-responsive polymer is herein proposed, which could offer new possibilities for the development of novel hydrogels that simultaneously exhibit the properties of both components. To this end, the synthetic biocompatible polypeptide PBLG and the thermo-responsive block PNIPAM were chosen as the main building blocks. Further modification and physical crosslinking of the polypeptide block allowed the desired hydrogel networks to be obtained, whose main physical properties are also investigated in the present work.

Experimental section

Materials

L-Glutamic acid γ-benzyl ester (Fluka, ≥99.0%), triphosgene (Aldrich, 98%), 1,3-propanediamine (PDA, Aldrich, ≥99%), *N*,*N*′-dicyclohexylcarbodiimide (DCC, Aldrich, 99%), *N*,*N*-dimethylformamide (DMF, Sigma-Aldrich, ≥99.8%, over molecular sieves), dichloromethane (DCM, Acros, 99.99%), tetrahydrofuran (THF, Sigma-Aldrich, 99.9%), methanol (Fluka, 99.8%), toluene (Fluka, ≥99.7%), diethyl ether (JBT, 99.5%), trifluoroacetic acid (TFA, Fluka, 98%), and hydrobromic acid in glacial acetic acid (Sigma-Aldrich, 33%) were used as received; ethyl acetate (Sigma-Aldrich, ≥99.9%) and cyclohexane (Sigma-Aldrich, ≥99.9%) were dried and distilled over CaH_2 (Fluka, >97.0%) at normal pressure. The α,ω-dicarboxy-terminated poly(*N*-isopropyl acrylamide) polymer (HOCO-PNIPAM-COOH) with a number average molecular mass of 35 500 g mol^{-1} and a polydispersity of 1.5 was purchased from Polymer Source Inc. and used as received. The diamino-terminated poly(ethylene oxide)-based crosslinker Jeffamine ED-2003 with an approximate number average molecular mass of 2300 g mol^{-1} was kindly provided by Huntsman Corporation and degassed before use.

Synthesis of the BLG-NCA monomer

γ-Benzyl L-glutamate *N*-carboxyanhydride (BLG-NCA) was synthesized according to previously published methods.[36] Briefly, in a 500 mL two-necked round-bottomed flask equipped with a magnetic stirrer, condenser, and nitrogen inlet, 15 g (63.2 mmol, 1 eq) of γ-benzyl L-glutamate and 8.13 g (27.4 mmol, 0.43 eq) of triphosgene were added and purged with nitrogen for 10 min. Freshly distilled ethyl acetate (250 mL) over CaH_2 was added, and the mixture was heated to 145 °C. After several hours (4 to 5 h), by checking the emission of HCl and total solution of the reacting mixture, the reaction was cooled down. The monomer was recrystallized from ethyl acetate/cyclohexane. Yield: 15.3 g (91%). ^{1}H NMR (360 MHz, acetone-d_6, δ): 7.98 (1H, s, N*H*), 7.26–7.43 (5H, m, Ar), 5.12 (2H, s, Ar–CH_2), 4.64 (1H, t, α-C*H*, J = 6.5 Hz), 2.63 (2H, t, γ-CH_2, J = 7.7 Hz), 2.45 (1H, m, β-C*H*), 2.14 (1H, m, β-C*H*) ppm. FTIR (ATR-diamond): 3256 (st, N–H), 3066 (st, ArC–H), 2936 (st, C–H), 1774 (st, C=O), 1703 (st, NC=O), 1254 (st, C–O), 930 (δ, ArC–C), 740 (γ, CH_2) cm^{-1}.

Synthesis of the H_2N-PNIPAM-NH_2 macroinitiator

The α,ω-diamino-terminated poly(*N*-isopropyl acrylamide) polymer (H_2N-PNIPAM-NH_2) was synthesized by reacting the corresponding α,ω-dicarboxy-terminated poly(*N*-isopropyl acrylamide) polymer (HOCO-PNIPAM-COOH) with an excess of 1,3-propanediamine (PDA) in the presence of *N*,*N*′-dicyclohexylcarbodiimide (DCC). In a 100 mL round-bottomed flask equipped with a magnetic stirrer and nitrogen inlet, 500 mg (0.014 mmol, 1 eq) of HOCO-PNIPAM-COOH and 14.5 mg (0.070 mmol, 2.5 eq) of DCC were added and purged with nitrogen for 10 min. DMF (50 mL) over molecular sieves and 25 mL (0.282 mmol, 10 eq) of PDA were added to the polymer solution. The mixture was stirred at room temperature for one day under an inert nitrogen atmosphere. The solvent and the excess PDA were evaporated at low pressure, and the resulting polymer was dissolved in THF. This polymer solution was filtered in order to remove the DCU by-product, and re-precipitated from DCM. The resulting polymer was freeze-dried for one day. Yield: 95%. ^{1}H NMR (360 MHz, methanol-d_4, δ): 7.47–8.20 (N*H*), 3.83–4.10 (CH_3–C*H*NH–CH_3), 1.26–2.36 (–CH_2–C*H*CO–), 1.02–1.26 (–CH_3) ppm. FTIR (ATR-diamond): 3251 (st, N–H), 2972 (st, C–H), 1633 (st, NC=O), 1540 (st sy, NHC=O; δ, N–H), 1458 (δ, CH_2 and CH_3), 1387 and 1367 (δ sy, CH_3), 1171 (γ, CH_3) cm^{-1}.

Synthesis of PBLG-*b*-PNIPAM-*b*-PBLG triblock copolymers

The α,ω-diamino-terminated poly(*N*-isopropyl acrylamide) macroinitiator (H_2N-PNIPAM-NH_2) and the γ-benzyl L-glutamate *N*-carboxyanhydride (BLG-NCA) monomer were dissolved at room temperature in separate dried flasks in DMF and under a nitrogen atmosphere. The monomer solution was transferred *via* syringe to the polymer solution. The mixture was stirred at room temperature for three days under an inert nitrogen atmosphere. After polymerization, the solvent was evaporated at low pressure. The resulting concentrated polymer solution was dissolved in THF and re-precipitated from DCM. After centrifugation and removal of the supernatant (three times), the resulting material was freeze-dried for one day. Yield: 80–90%. ^{1}H NMR (360 MHz, $CDCl_3$, δ): 7.95–8.70 (^{i}Pr–N*H*CO– and –CH–N*H*CO–), 7.15–8.42 (Ar), 4.89–5.20 (Ar–CH_2), 3.69–4.23 (α-C*H* and CH_3–C*H*NH–CH_3), 1.26–2.80 (β-CH_2, γ-CH_2 and –CH_2–C*H*CO–), 1.02–1.26 (–CH_3) ppm. FTIR (ATR-diamond): 3289 (st, N–H), 3066 (st, Ar–C–H), 2973 (st, C–H), 1730 (st, C=O), 1649 (st, NC=O), 1543 (st sy, NHC=O; δ, N–H), 1453 (δ, CH_2 and CH_3), 1388 and 1367 (δ sy, CH_3), 1163 (γ, CH_3), 969 (δ ip, ArC–H), 736 and 696 (δ oop, ArC–H) cm^{-1}.

Synthesis of PLGA-*b*-PNIPAM-*b*-PLGA triblock copolymers

The deprotection of the benzyl groups was carried out as follows: in a 25 mL round-bottomed flask, the triblock copolymer (PBLG-*b*-PNIPAM-*b*-PBLG) was dissolved in 1 mL of trifluoroacetic acid (TFA) at 0 °C, and 0.5 mL of hydrobromic acid in glacial acetic acid was added, keeping the reaction at room temperature for 2 h. The polymer was precipitated by adding diethyl ether, and the solvents were removed under vacuum. The resulting triblock copolymer (PLGA-*b*-PNIPAM-*b*-PLGA) was dried at low pressure at room temperature for 24 h. Yield: 95%. ^{1}H NMR (400 MHz, DMSO-d_6, δ): 6.90–8.75 (^{i}Pr–N*H*CO–, –CH–N*H*CO– and COO*H*), 3.67–4.10 (α-C*H* and CH_3–C*H*NH–CH_3), 1.16–2.41 (β-CH_2, γ-CH_2 and –CH_2–C*H*CO–), 0.90–1.16 (–CH_3) ppm. FTIR (ATR-diamond): 3268 (st, N–H), 3068 (st, COO–H), 2974 (st, C–H), 1710 (st, C=O), 1636 (st, NC=O), 1541 (st sy, NHC=O; δ, N–H), 1452 (δ, CH_2 and CH_3), 1389 and 1368 (δ sy, CH_3), 1168 (γ, CH_3) cm^{-1}.

Preparation of the ionic complexes

Complexes of each PLGA-*b*-PNIPAM-*b*-PLGA triblock copolymer with the diamino-terminated polyether Jeffamine ED-2003 were prepared by mixing solutions of both components in *N*,*N*-dimethylformamide (DMF) at a molar ratio of 1 : 10 (PLGA : PEO). After slow evaporation of the solvent under vacuum at room temperature for 10 days, the final network samples were obtained and ready to use for further experiments. FTIR (ATR-diamond): 3289 (st, N–H), 3063 (st, COO–H), 2969 (st, C–H), 2876 (st, OC–H), 1722 (st, C=O), 1650 (st, NC=O), 1546 (st sy, NHC=O; δ, N–H), 1456 (δ, (O)CH_2 and (O)CH_3), 1386 and 1344 (δ sy, CH_3), 1103 (γ, OCH_2), 956 and 841(γ, CH_2) cm^{-1}.

Swelling behaviour of the ionic complexes

Swelling experiments were carried out at 25 and 40 °C by keeping the sample in a water atmosphere generated from pure water (equilibrium relative humidity 100%), KCl–water (equilibrium relative humidity 84.34%), and NaCl–water (equilibrium relative humidity 75.29%). The swelling ratio of the networks was calculated by using the following formula: $\Delta m(\%) = (m_s - m_d)/m_d \times 100$, where m_d and m_s denote the mass of the dry and swollen ionic complexes, respectively.

Techniques and apparatus

^{1}H NMR and 2D ^{1}H–^{1}H cosy-NMR measurements were carried out at room temperature on a Bruker DPX-360 spectrometer operating at 360 MHz or on a Bruker Avance Spectrometer operating at 400 MHz, and using acetone-d_6, methanol-d_4, DMSO-d_6 or $CDCl_3$ as solvents and as the internal standards. Fourier transform infrared (FTIR) spectra of solid samples were recorded at room temperature with a Varian 640 FTIR spectrometer and using a MKII golden gate single attenuated total reflection (ATR) system in the spectral region from 600 to 4000 cm^{-1} with 4 cm^{-1} resolution. Circular Dichroism (CD) experiments were performed on a Jasco-815 spectrometer at room temperature. The triblock copolymers were cast from their corresponding DMF solutions on a quartz substrate, and measured in the wavelength range from 190 to 290 nm at a scanning speed of 100 nm min^{-1}. Small and Wide-Angle X-ray Scattering (SAXS & WAXS) measurements were performed using an Anton-Paar SAXSess diffractometer with a fine line focus sealed copper tube (PANalytical, PW 3830) and a Rigaku MicroMax-002+ microfocused beam (4 kW, 45 kV, 0.88 mA) to obtain direct information on the high scattering vector ranges, respectively. The CuK_α radiation ($\lambda_{CuK\alpha} = 1.5418$ Å) was filtered by a Göbel mirror and a Kratky block collimation system (Anton-Paar SAXSess) and collimated by three pinhole (0.4, 0.3, and 0.8 mm) collimators (Rigaku MicroMax-002+). The scattered X-ray intensity was collected on a Packard Cyclone storage phosphor screen image plate (200 × 66 mm, 50 × 50 μm per pixel resolution) – Anton-Paar SAXSess – or detected by a Fuji Film BAS-MS 2025 imaging plate system (15.2 × 15.2 cm^2, 50 mm resolution) – Rigaku MicroMax-002+. The background from mica foil used to clamp the samples was subtracted from the diffractograms. An effective scattering-vector range of 0.5 nm^{-1} < q < 25 nm^{-1} was obtained, where q is the scattering wave-vector defined as $q = 4\pi \sin(\theta)/\lambda_{CuK\alpha}$, with a scattering angle of 2θ.

Results and discussion

In order to obtain a series of novel thermo-responsive peptide based hydrogels, the BLG-NCA monomer – γ-benzyl L-glutamate *N*-carboxyanhydride – was synthesized using the method previously published.[36] The diamino-terminated PNIPAM homopolymer – H_2N-PNIPAM-NH_2 – was obtained by reacting the dicarboxy-terminated PNIPAM homopolymer – HOOC-PNIPAM-COOH – with an excess of 1,3-propanediamine (PDA) in the presence of *N*,*N*′-dicyclohexylcarbodiimide (DCC). The resulting diamino-terminated macroinitiator was reacted with controlled quantities of the BLG-NCA monomer *via* ring opening polymerization (ROP),[36–39] and three different triblock copolymers with various degrees of polymerization of the PBLG block were synthesized, as shown in Scheme 1, by controlling the ratio between the BLG-NCA monomer and the macroinitiator. The resulting triblock copolymers (PBLG-*b*-PNIPAM-*b*-PBLG) – P1, P2 and P3 – were characterized by ^{1}H NMR (Fig. 1), FTIR and WAXS experiments (Fig. ESI-1†), showing an α-helix conformation of the polypeptide block due to the presence of two absorption peaks at $\nu = 1649$ and 1543 cm^{-1} (amide I and II stretching vibrational bands) and, in bulk, the perfectly sharp peaks at $q_1 = 4.7$ nm^{-1} ($d = 1.33$ nm) and $q_2 = 8.3$ nm^{-1} which correspond to the hexagonal packing of α-helices in the solid state.

The benzyl protecting groups were successfully removed by the deprotection method previously published.[37] The resulting triblock copolymers (PLGA-*b*-PNIPAM-*b*-PLGA) – DP1, DP2 and DP3 – were characterized by ^{1}H NMR and FTIR (Fig. ESI-2†), maintaining the same degree of polymerization with the complete removal of benzyl protecting groups (Scheme 1). Table 1 summarizes all the information concerning the number average molecular mass (M_n), the average degree of polymerization (DP_{PBLG}) of one polypeptide segment, and the volume fraction (ϕ_{PBLG}) of the two polypeptide segments of these three triblock copolymers and the corresponding deprotected ones.

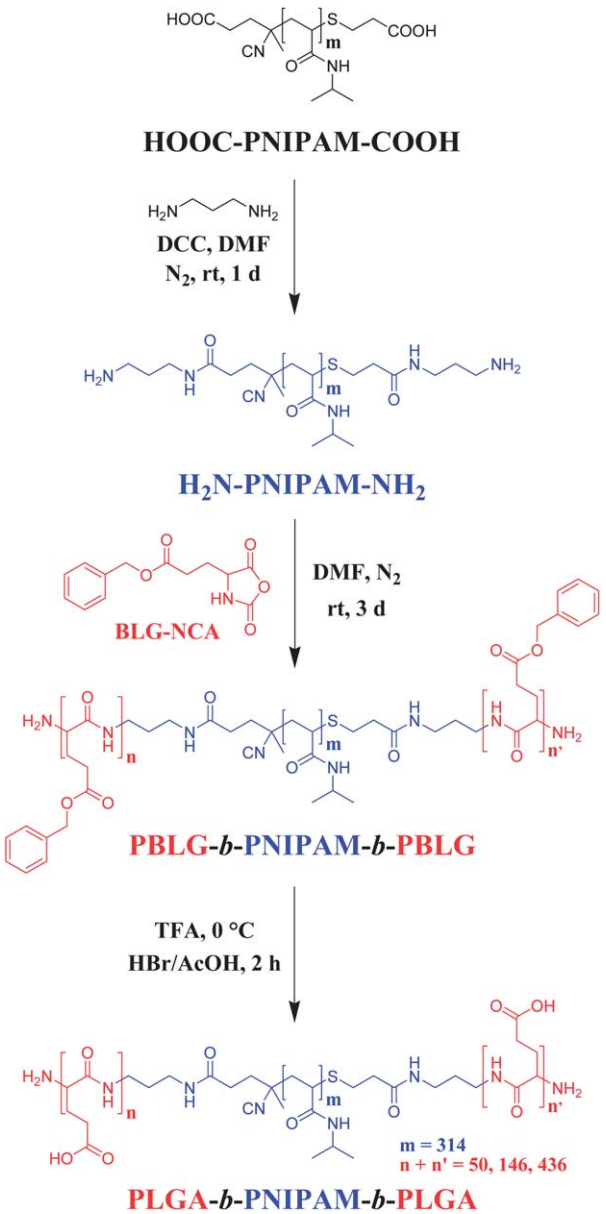

Scheme 1 Synthetic route for the preparation of the PLGA-*b*-PNIPAM-*b*-PLGA triblock copolymers.

The physically crosslinked ionic complexes were prepared from an organic solvent (DMF) *via* acid–base proton transfer between the triblock copolymer (PLGA-*b*-PNIPAM-*b*-PLGA) and diamino terminated PEO crosslinker at a ratio of 1 : 10 (PLGA to PEO). After removing the solvent under vacuum at room temperature, the resulting triblock copolymer-based ionic complexes – IC1, IC2 and IC3 – were further characterized by means of FTIR spectroscopy (Fig. ESI-2†).

In order to confirm the complexation through acid–base proton transfer from the carboxylic acid from the polypeptide block PLGA to the amino group from the PEO crosslinker, FTIR experiments were performed on the triblock copolymers – DP1, DP2 and DP3 – before and after complexation – IC1, IC2 and IC3. The results showed the presence of the secondary structure of the peptide block, which corresponds to the common α-helix,

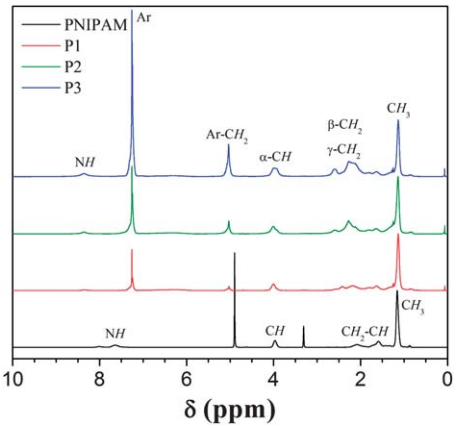

Fig. 1 ^{1}H NMR spectra of the PNIPAM homopolymer and the three PBLG-*b*-PNIPAM-*b*-PBLG triblock copolymers P1, P2 and P3.

with a small change in the absorption peak positions of the stretching vibrational bands of both amide I and II (Fig. 2a). Before complexation the absorption peak was located at 1636 and 1541 cm^{-1}, and after complexation both peaks appeared at 1650 and 1546 cm^{-1}, respectively. Moreover, before complexation, one absorption peak was observed at 1710 cm^{-1} belonging to the stretching vibrational band from the carboxylic acid (COOH), which shifted to 1722 cm^{-1} when carboxylates (COO^-) are present in the sample after proton transfer to the amino group from the PEO crosslinker. Due to the ion pair formation by acid–base proton transfer, one absorption peak appeared at 1345 cm^{-1}, which belongs to the ammonium group from the PEO crosslinker (NH_3^+).[40,41] Similar behaviour was also observed for the other two ionic complexes IC1 and IC2 (Fig. ESI-2†).

Furthermore, in order to understand the role of the secondary structure of the peptide block in the triblock copolymer and its corresponding ionic complex, solid-state CD experiments were performed on all triblock copolymers before – DP1, DP2 and DP3 – and after complexation – IC1, IC2 and IC3. In both cases, before and after complexation, the typical pattern for an α-helix conformation was observed as shown in Fig. 2b, with two minima peaks around 211 and 223 nm, which correspond to the π–π* and n–π* transitions, respectively.[37,42] These results confirm the maintenance of the secondary structure in the polypeptide block before and after deprotection, and before and after complexation.

The swelling behaviour of the ionic complexes was investigated by recording the water uptake by the network over time until reaching equilibrium: $\Delta m(\%) = (m_s - m_d)/m_d \times 100$, where m_d and m_s denote the mass of the dry and swollen ionic complexes, respectively. All the experiments were performed in a water atmosphere where the equilibrium relative humidity was controlled by means of temperature and water composition – pure water, KCl–water and NaCl–water. The method involving vapor sorption isotherms was preferred to the one relying on weight changes upon immersion in liquid water only for a matter of measurements precision. Additional experiments were carried out in liquid water (not shown) which indicated, as expected, a sharp swelling upon immersion in liquid water at

Table 1 Number average molecular mass (M_n), average degree of polymerization (DP_{PBLG}) for a single PBLG segment, volume fraction (ϕ_{PBLG}) of the two PBLG segments, and theoretical length of the peptide segment (L_α) in the α-helix conformation for the PBLG-*b*-PNIPAM-*b*-PBLG and the corresponding deprotected PLGA-*b*-PNIPAM-*b*-PLGA (in parentheses) triblock copolymers

Sample	Block composition	M_n[a] (g mol^{-1})	DP_{PBLG}[a]	ϕ_{PBLG}[b]	L_α[c] (nm)
P1 (DP1)	$PBLG_{25}$-$PNIPAM_{314}$-$PBLG_{25}$ ($PLGA_{25}$-$PNIPAM_{314}$-$PLGA_{25}$)	46 500 (42 000)	25	0.25 (0.18)	3.8
P2 (DP2)	$PBLG_{73}$-$PNIPAM_{314}$-$PBLG_{73}$ ($PLGA_{73}$-$PNIPAM_{314}$-$PLGA_{73}$)	67 500 (54 400)	73	0.50 (0.37)	11.0
P3 (DP3)	$PBLG_{218}$-$PNIPAM_{314}$-$PBLG_{218}$ ($PLGA_{218}$-$PNIPAM_{314}$-$PLGA_{218}$)	131 100 (91 800)	218	0.75 (0.63)	32.7

[a] Calculated by ^{1}H NMR. [b] Calculated from the following equation: $\phi_{PBLG} = M_{n,PBLG} \times \rho_{PBLG}^{-1}/(M_{n,PBLG} \times \rho_{PBLG}^{-1} + M_{n,PNIPAM} \times \rho_{PNIPAM}^{-1})$, where $\rho_{PBLG} = 1.278$ g cm^{-3} and $\rho_{PNIPAM} = 1.386$ g cm^{-3}, and $\rho_{PLGA} = 1.526$ g cm^{-3} for the corresponding deprotected triblock copolymers. [c] Calculated from the following equation: $L_\alpha = 0.15 DP_{PBLG}$.

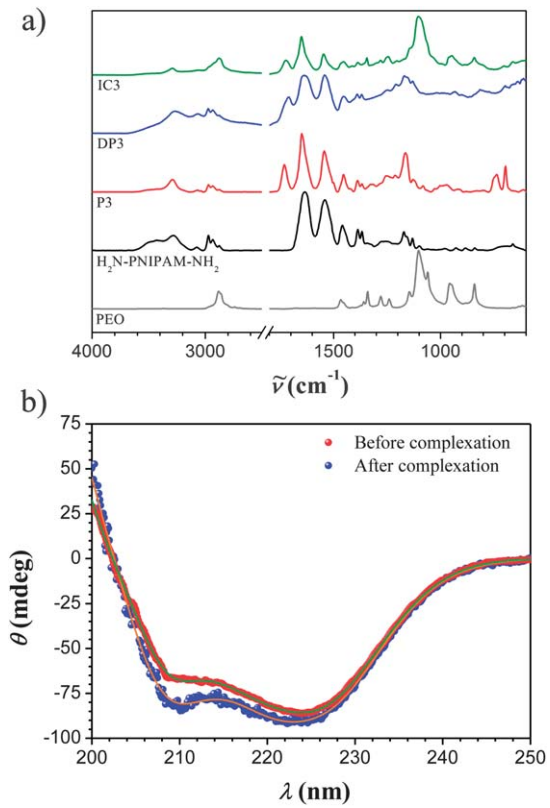

Fig. 2 (a) FTIR spectra of the diamino-terminated PEO crosslinker, the diamino-terminated PNIPAM homopolymer, the PBLG-*b*-PNIPAM-*b*-PBLG triblock copolymer P3, the PLGA-*b*-PNIPAM-*b*-PLGA triblock copolymer DP3, and the ionic complex IC3. (b) Circular dichroism spectra of the PLGA-*b*-PNIPAM-*b*-PLGA triblock copolymer DP3 and its corresponding ionic complex IC3.

room temperature, and this, without any dissolution, confirming the physical nature of the hydrogels. Temperatures of 25 °C and 40 °C were chosen in order to study the effect of temperature on the swelling capacity of the networks since sorption and desorption of water molecules should be expected below and above the LCST of the thermo-responsive PNIPAM block. Fig. 3a shows the swelling behaviour of the ionic complex IC3 at 25 °C and 40 °C, and at different equilibrium relative humidities. The ionic complex swells much more at 25 °C than at 40 °C because of the hydrophobic behaviour of the PNIPAM block above its LCST, conditions at which only the hydrophilic PEO segments are mainly responsible for the water uptake. When comparing the swelling behaviour of the ionic complexes at different equilibrium relative humidities, a clear tendency was observed. The networks swelled the most in a pure water atmosphere (ERH = 100%), followed by KCl–water (ERH = 84.34%) and NaCl–water (ERH = 75.29%) atmospheres. Similar behaviour was also observed for the other two ionic complexes IC1 and IC2 (Fig. ESI-4†).

In order to obtain further insight into the swelling kinetics of the networks and estimate the equilibrium swelling ratio, all experiments were fitted using the Weibull model[43–45] for water sorption (eqn (1), stretched exponential growth) and for water desorption (eqn (2), stretched exponential decay):

$$\Delta m = \Delta m_0 + \Delta m_{eq}\left(1 - e^{-\left(\frac{t-t_0}{\tau_s}\right)^{\beta_s}}\right) \quad (1)$$

$$\Delta m = \Delta m_{eq} + \Delta m_0 e^{-\left(\frac{t-t_0}{\tau_d}\right)^{\beta_d}} \quad (2)$$

where Δm, Δm_0 and Δm_{eq} are the swelling ratio, the initial swelling ratio and the equilibrium swelling ratio, respectively. The two kinetic factors – for swelling τ_s and β_s, and for deswelling τ_d and β_d – are, respectively, the lifetime and the stretching factor.

In order to compare the results from the swelling experiments (Fig. ESI-5 and Tables ESI-1–ESI-3†), and since the three ionic complexes have different hydrophilic fraction compositions, the equilibrium swelling ratio Δm_{eq} was normalized with respect to the water uptake components for each sample. Thus, for the networks at 25 °C, the PEO and the PNIPAM blocks are mainly responsible for the swelling of the ionic complex, and the corresponding hydrophilic fractions are $\phi_w = 0.88$, 0.79 and 0.71 for the samples IC1, IC2 and IC3, respectively. At 40 °C, above the LCST of the PNIPAM block, the PEO segment is the only component contributing to the water uptake, and the corresponding hydrophilic fractions are $\phi_w = 0.22$, 0.38 and 0.5 for the networks IC1, IC2 and IC3, respectively (Fig. 3b). It is worth noting that a quick equilibrium calculation indicates that the polyelectrolytic nature of the PLGA block is nearly entirely suppressed (PLGA remains protonated) in highly concentrated polymer solutions/hydrogels, due to the weak nature of this polyelectrolyte (Fig. ESI-6†), and thus, this block does not contribute to the hydrophilic phase of the hydrogel.

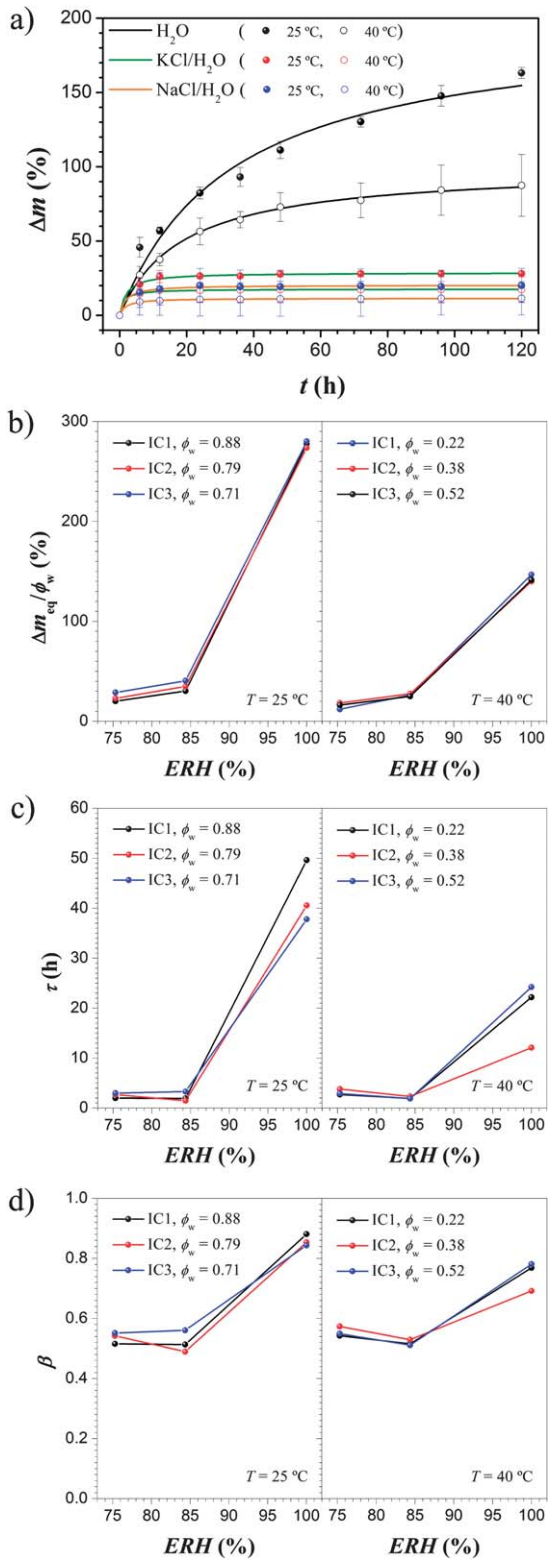

Fig. 3 (a) Swelling behaviour of the ionic complex IC3 at 25 °C and 40 °C in water, KCl–water, and NaCl–water atmospheres. (b) Equilibrium swelling ratio normalized to the hydrophilic fraction ($\Delta m_{eq}/\phi_w$), (c) swelling lifetime (τ), and (d) swelling stretching factor (β) for the three ionic complexes IC1, IC2 and IC3 at 25 °C and 40 °C in water, KCl–water, and NaCl–water atmospheres. Water: black symbols; KCl–water: red symbols; NaCl–water: blue symbols.

The normalized equilibrium swelling ratios $\Delta m_{eq}/\phi_w$ are nearly identical for the samples at 25 °C, which indicates that the maximum adsorbed water is controlled directly by the PEO and PNIPAM blocks volume fraction. The only difference remains in the values achieved at different equilibrium relative humidities (ERH), which decrease when the water content in the air is lowered. At 40 °C, since the PNIPAM block is no longer adsorbing water, the normalized equilibrium swelling ratios are lower compared to those obtained at 25 °C, yet remaining nearly identical for the different hydrogels at any specific relative humidity.

The analysis of the kinetic factors such as the lifetime τ and the stretching factor β (Fig. 3c and 3d) shows how fast the water uptake process is depending on the equilibrium relative humidity and how much the mass time evolution deviates from a pure exponential behaviour. In general, the swelling kinetics were faster at 40 °C than at 25 °C. At low equilibrium relative humidity, ERH, the swelling process at 25 °C was 12 to 25 times faster than at 100% ERH, while at 40 °C the process was 4 to 12 times faster, which indicates a faster process at low ERH values. With respect to the stretching factor β, values of 0.50–0.60 were obtained for low equilibrium relative humidity and values of 0.70–0.90 at 100% ERH.

Moreover, in order to understand the sorption and desorption behaviour of these ionic complexes, cyclic swelling–deswelling experiments on the network IC3 were performed. The sample was swollen at 25 °C in a pure water atmosphere and, afterwards, warmed to 40 °C. Fig. 4 shows the swelling and deswelling cycles of the ionic complex IC3. All processes were analyzed by fitting the curves with eqn (1) for the sorption process and eqn (2) for the desorption process, and all calculated parameters are shown in Table 2. The kinetics at 25 °C, during the swelling process, are faster than at 40 °C when water is desorbed from the polymer network. The most important result is that the sample shows reversible thermal-responsiveness due to the desorption of water when heating the sample above the LCST of the PNIPAM, and fast swelling–deswelling processes can be easily and reiteratively achieved in water media, which might be interesting for drug release experiments.

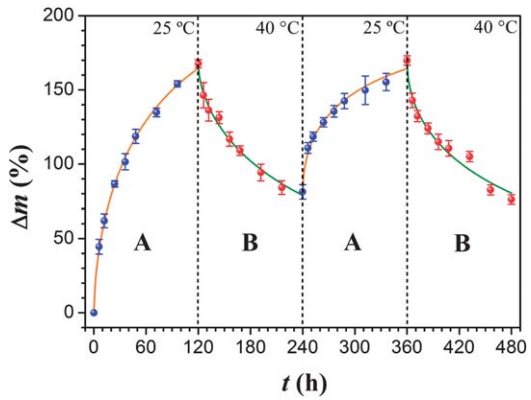

Fig. 4 Swelling and deswelling cycles of the ionic complex IC3 in a water atmosphere at 25 °C and 40 °C.

Table 2 Swelling (25 °C) and deswelling (40 °C) cycle parameters of the ionic complex IC3 in a water atmosphere

	Δm_{eq} (%)	Δm_0 (%)	τ (h)	β
1st swelling	169 ± 11	0	35.4 ± 0.3	0.83 ± 0.01
1st deswelling	51 ± 14	165 ± 14	78 ± 12	0.75 ± 0.04
2nd swelling	163 ± 7	81 ± 1	26.7 ± 0.2	0.78 ± 0.01
2nd deswelling	51 ± 10	168 ± 5	78 ± 10	0.62 ± 0.04

The analysis of the X-ray pattern of the ionic complex IC3 in dry state and in wet state revealed the presence of the micro-phase separated hexagonal packing of α-helices from the PLGA rods (Fig. 5). The dry network shows three sharp peaks at $q_1 = 3.79$ nm^{-1}, $q_2 = 6.56$ nm^{-1} and $q_3 = 7.60$ nm^{-1} and two characteristic sharp peaks coming from the crystalline PEO segments at $q_{PEO} = 13.4$ and 16.3 nm^{-1}, while the swollen network at 25 °C only has peaks at $q_1 = 3.67$ nm^{-1}, $q_2 = 6.41$ nm^{-1} and $q_3 = 7.76$ nm^{-1}. Therefore, the disappearance of the two PEO peaks in the swollen network clearly indicates the swelling of the PEO domains. Thus, at 25 °C, the hydrophobic PLGA block works as a physical crosslinker and phase separates from the rest of the components, which adsorb water.

When heating up the sample at 40 °C, the PNIPAM block becomes water incompatible, and water is reversibly released from the hydrogel PNIPAM domains establishing a new water content isothermal equilibrium. The swollen network at 40 °C shows the hexagonal packing of α-helices with the three peaks at $q_1 = 3.80$ nm^{-1}, $q_2 = 6.56$ nm^{-1} and $q_3 = 7.89$ nm^{-1}, which indicate the swollen PLGA-PEO domains while the PNIPAM domains are deswollen (Fig. 6).

In order to confirm the swelling–deswelling processes from the PNIPAM domains, SAXS experiments were performed on the swollen ionic complex IC3 at 20 °C and 40 °C (Fig. 7). The results show a broad peak which shifts from $q = 0.22$ nm^{-1} to 0.70 nm^{-1} when the sample is swollen at 20 and 40 °C, respectively. This peak shifting indicates an anisotropic reduction of the distance between the PLGA-rich domains when PNIPAM collapses upon reaching its LCST and water is expelled from the PNIPAM domains.

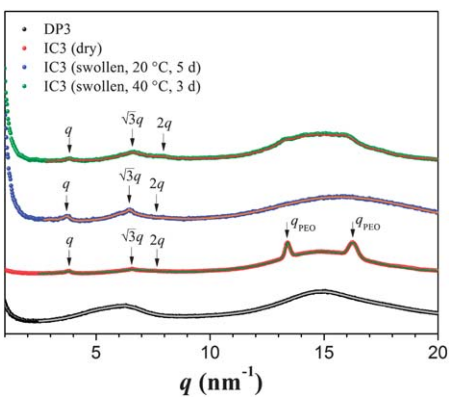

Fig. 5 WAXS patterns of the PLGA-*b*-PNIPAM-*b*-PLGA triblock copolymer DP3, the corresponding ionic complex IC3 in dry state, and in swollen state at 20 °C and 40 °C.

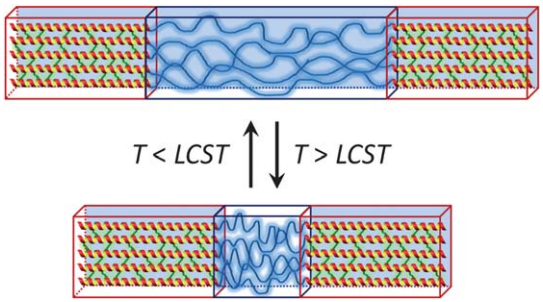

Fig. 6 Schematic illustration showing the thermal-responsiveness of the peptide-based triblock copolymer hydrogel.

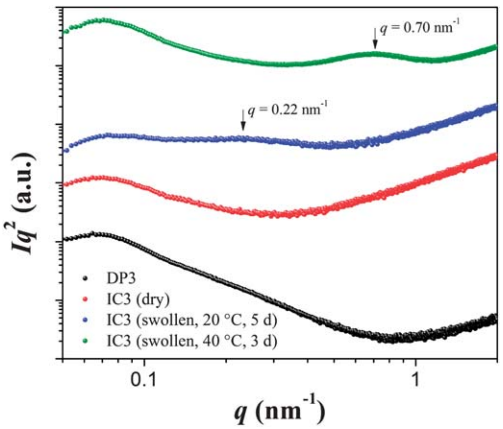

Fig. 7 SAXS patterns of the PLGA-*b*-PNIPAM-*b*-PLGA triblock copolymer DP3, the corresponding ionic complex IC3 in dry state, and in swollen state at 20 °C and 40 °C.

Conclusions

A new series of rod-coil-rod peptide-based triblock copolymers which contain a thermo-responsive coil block have been synthesized and complexes were obtained by acid–base proton transfer between the carboxylic acid groups from the peptide block and the amine groups from a hydrophilic polyether crosslinker. The resulting ionic complexes absorb water from the atmosphere and behave as thermo-responsive hydrogels. The equilibrium swelling ratio of these hydrogels increases with increasing equilibrium relative humidity and decreasing temperature. Moreover, the kinetics of the swelling process are faster at low equilibrium relative humidity and at high temperatures. Given the biocompatibility of all components and the temperature responsiveness of the system, which allows iterative and fast sorption–desorption cycles of water, these peptide-based hydrogels show promise in biotechnological and biomedical applications, such as tissue engineering and injectable materials for drug delivery.

Acknowledgements

This work was carried out with the financial support of the FRIMAT center for Nanomaterials and the Swiss Science National Foundation.

Notes and references

1 S. Van Vlierberghe, P. Dubruel and E. Schacht, *Biomacromolecules*, 2011, **12**, 1387–1408.
2 N. A. Peppas, P. Bures, W. Leobandung and H. Ichikawa, *Eur. J. Pharm. Biopharm.*, 2000, **50**, 27–46.
3 J. L. Drury and D. J. Mooney, *Biomaterials*, 2003, **24**, 4337–4351.
4 W. E. Hennink and C. F. van Nostrum, *Adv. Drug Delivery Rev.*, 2002, **54**, 13–36.
5 A. S. Hoffman, *Adv. Drug Delivery Rev.*, 2002, **54**, 3–12.
6 A. M. Jonker, D. W. P. M. Löwik and J. C. M. van Hest, *Chem. Mater.*, 2011, **24**, 759–773.
7 C. T. Huynh, M. K. Nguyen and D. S. Lee, *Macromolecules*, 2011, **44**, 6629–6636.
8 I. Kosif, E. J. Park, R. Sanyal and A. Sanyal, *Macromolecules*, 2010, **43**, 4140–4148.
9 E. S. Gil and S. M. Hudson, *Prog. Polym. Sci.*, 2004, **29**, 1173–1222.
10 L. E. Bromberg and E. S. Ron, *Adv. Drug Delivery Rev.*, 1998, **31**, 197–221.
11 B. Jeong, S. W. Kim and Y. H. Bae, *Adv. Drug Delivery Rev.*, 2002, **54**, 37–51.
12 D. Schmaljohann, *Adv. Drug Delivery Rev.*, 2006, **58**, 1655–1670.
13 T. Miyata, T. Uragami and K. Nakamae, *Adv. Drug Delivery Rev.*, 2002, **54**, 79–98.
14 M. K. Nguyen and D. S. Lee, *Macromol. Biosci.*, 2010, **10**, 563–579.
15 L. Yu and J. Ding, *Chem. Soc. Rev.*, 2008, **37**, 1473–1481.
16 H. Feil, Y. H. Bae, J. Feijen and S. W. Kim, *Macromolecules*, 1993, **26**, 2496–2500.
17 M. A. Ward and T. K. Georgiou, *Polymers*, 2011, **3**, 1215–1242.
18 M. Prabaharan and J. F. Mano, *Macromol. Biosci.*, 2006, **6**, 991–1008.
19 A. Carlsen and S. Lecommandoux, *Curr. Opin. Colloid Interface Sci.*, 2009, **14**, 329–339.
20 F. Chécot, A. Brûlet, J. Oberdisse, Y. Gnanou, O. Mondain-Monval and S. Lecommandoux, *Langmuir*, 2005, **21**, 4308–4315.
21 E. P. Holowka, D. J. Pochan and T. J. Deming, *J. Am. Chem. Soc.*, 2005, **127**, 12423–12428.
22 M. Bikram, C. Ahn, S. Y. Chae, M. Lee, J. W. Yockman and S. W. Kim, *Macromolecules*, 2004, **37**, 1903–1916.
23 A. Pal, S. Shrivastava and J. Dey, *Chem. Commun.*, 2009, 6997–6999.
24 R. A. Stile and K. E. Healy, *Biomacromolecules*, 2001, **2**, 185–194.
25 P. Markland, Y. Zhang, G. L. Amidon and V. C. Yang, *J. Biomed. Mater. Res.*, 1999, **47**, 595–602.
26 M. Suzuki, T. Sato, A. Kurose, H. Shirai and K. Hanabusa, *Tetrahedron Lett.*, 2005, **46**, 2741–2745.
27 D. J. Pochan, J. P. Schneider, J. Kretsinger, B. Ozbas, K. Rajagopal and L. Haines, *J. Am. Chem. Soc.*, 2003, **125**, 11802–11803.
28 J. P. Schneider, D. J. Pochan, B. Ozbas, K. Rajagopal, L. Pakstis and J. Kretsinger, *J. Am. Chem. Soc.*, 2002, **124**, 15030–15037.
29 V. Breedveld, A. P. Nowak, J. Sato, T. J. Deming and D. J. Pine, *Macromolecules*, 2004, **37**, 3943–3953.
30 A. P. Nowak, V. Breedveld, L. Pakstis, B. Ozbas, D. J. Pine, D. Pochan and T. J. Deming, *Nature*, 2002, **417**, 424–428.
31 M. H. Park, M. K. Joo, B. G. Choi and B. Jeong, *Acc. Chem. Res.*, 2012, **45**, 424–433.
32 F. Horkay, I. Tasaki and P. J. Basser, *Biomacromolecules*, 2001, **2**, 195–199.
33 K. Nam, J. Watanabe and K. Ishihara, *Int. J. Pharm.*, 2004, **275**, 259–269.
34 X. Qu, A. Wirsen and A. C. Albertsson, *J. Appl. Polym. Sci.*, 1999, **74**, 3186–3192.
35 Y. Chen, X. Pang and C. Dong, *Adv. Funct. Mater.*, 2010, **20**, 579–586.
36 A. Sánchez-Ferrer and R. Mezzenga, *Macromolecules*, 2010, **43**, 1093–1100.
37 V. K. Kotharangannagari, A. Sánchez-Ferrer, J. Ruokolainen and R. Mezzenga, *Macromolecules*, 2011, **44**, 4569–4573.
38 M. R. Hammond, H. A. Klok and R. Mezzenga, *Macromol. Rapid Commun.*, 2008, **29**, 299–303.
39 V. K. Kotharangannagari, A. Sánchez-Ferrer, J. Ruokolainen and R. Mezzenga, *Macromolecules*, 2012, **45**, 1982–1990.
40 A. M. Sukhotin, *Problems of the Theory of Solutions of Electrolytes in Media with a Low Dielectric Constant*, Goskhimizdat, Moscow, 1959.
41 J. W. Smith and M. C. Vitoria, *J. Chem. Soc. A*, 1968, 2468–2474.
42 H. Block, *Poly (γ-Benzyl L-Glutamate) and Other Glutamic Acid Containing Polymers*, Gordon and Breach, New York, 1983.
43 P. García-Pascual, N. Sanjuan, R. Melis and A. Mulet, *J. Food Eng.*, 2006, **72**, 346–353.
44 M. F. Machado, F. A. R. Oliveira and L. M. Cunha, *Int. J. Food Sci. Technol.*, 1999, **34**, 47–57.
45 A. Marabi, S. Livings, M. Jacobson and I. S. Saguy, *Eur. Food Res. Technol.*, 2003, **217**, 311–318.